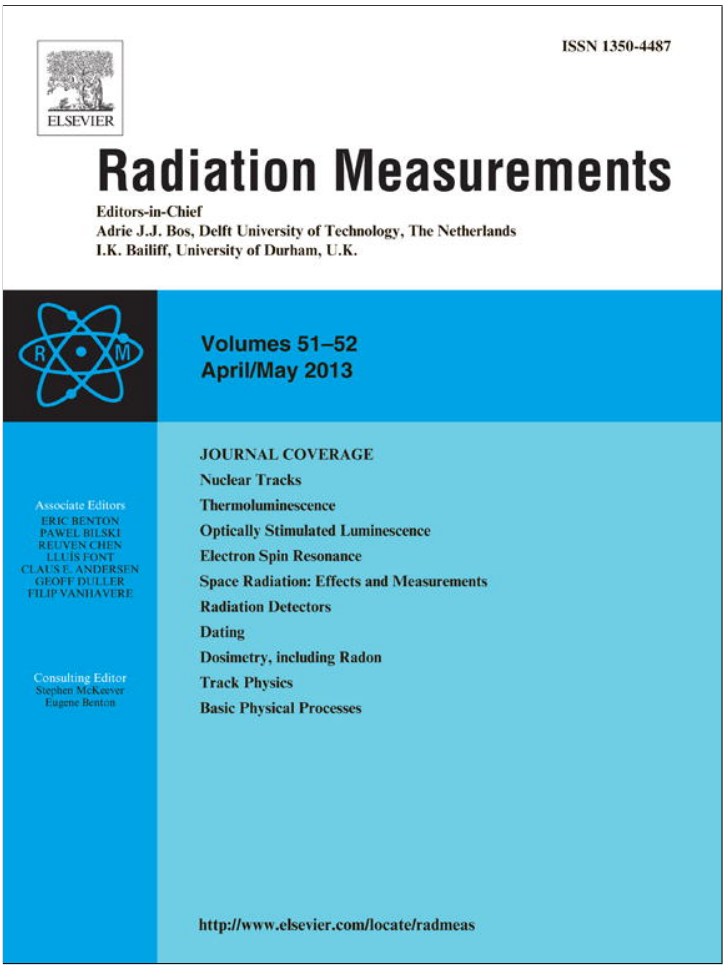

Radiation Measurements 51-52 (2013) 40–47

Contents lists available at SciVerse ScienceDirect

Radiation Measurements

journal homepage: www.elsevier.com/locate/radmeas

Anomalous heating rate effect in thermoluminescence intensity using a simplified semi-localized transition (SLT) model

Vasilis Pagonis*, Leigh Blohm, Mark Brengle, Gina Mayonado, Patrick Woglam

Physics Department, McDaniel College, 2 College Hill, Westminster, MD 21157, USA

HIGHLIGHTS

- Anomalous heating rate phenomenon of TL is explained with simplified SLT model.
- 2000 random variations of parameters in the model are simulated.
- Variable heating rate method systematically underestimates activation energy *E*.
- Relevance to experimental work on double doped dosimetric material YPO_4.

ARTICLE INFO

Article history:
Received 30 October 2012
Received in revised form
28 January 2013
Accepted 31 January 2013

ABSTRACT

During thermoluminescence (TL) measurements carried out with different heating rates, one expects the total number of emitted photons to be constant. However, for many luminescence materials one observes a decreased intensity of luminescence at elevated temperatures, due to the presence of the well-known phenomenon of thermal quenching. Recent experimental work on the dosimetric material YPO_4 double doped with lanthanides demonstrated the exact opposite behavior, in which the total luminescence intensity increases with the heating rate during the TL experiments. This anomalous TL behavior was recently explained by using the Mandowski model of semi-localized transitions (SLTs). In this paper it is shown that this anomalous heating rate or "anti-quenching" phenomenon can also be described by using a simplified SLT model of TL with approximated kinetic equations. The simulated glow curves show that as the probability of the non-radiative processes increases, the anomalous heating rate effect becomes dominant. The dependence of the anomalous heating rate effect on the values of the kinetic parameters in the model is examined by allowing random variations of the parameters in the model, within wide ranges of physically reasonable values covering several orders of magnitude. It is shown by simulation that the variable heating rate method can systematically underestimate the value of the activation energy *E*, while by contrast the initial rise method of analysis almost always yields the correct *E* value. These simulated results are discussed in relation to recent experimental work on the double doped dosimetric material YPO_4.

1. Introduction

Three commonly used theoretical models of thermoluminescence (TL) are the single trap model (STM), localized transition (LT) models and semi-localized transition (SLT) kinetic model. The STM model assumes a uniform spatial distribution of traps and recombination centers, while LT models are based on the existence of electron–hole pairs trapped close to each other. The SLT models assume a spatial correlation of traps (T) and recombination centers (RC), and are thought to be applicable to physical situations where the excitation is carried out by high-energy radiation, so that traps and recombination centers are populated along tracks (see for example Chen and Pagonis (2011), and references therein).

A number of works have dealt with the SLT model of TL (see: Pagonis and Kulp, 2010; Mandowski, 2008, 2005; Kumar et al., 2006, 2007; Pagonis, 2005; Horowitz et al., 2003). Mandowski (2006, 2008) examined spatially correlated systems of traps and recombination centers, and showed that these are responsible for many anomalous TL phenomena, like the existence of smaller peaks in the TL glow curves called the displacement peaks, the occurrence of very high frequency factors associated with the mechanism of cascade detrapping (CD), and the anomalous heating rate effect (Mandowski and Bos, 2011).

* Corresponding author. Tel.: +1 410 857 2481; fax: +1 410 386 4624.
E-mail address: vpagonis@mcdaniel.edu (V. Pagonis).

1350-4487/$ – see front matter © 2013 Elsevier Ltd. All rights reserved.
http://dx.doi.org/10.1016/j.radmeas.2013.01.025

Recently the SLT model has attracted attention in connection with the TL properties of YPO_4 doped with trivalent lanthanide ions (Mandowski and Bos, 2011). The effect of heating rate on TL glow curves is commonly used to determine trap parameters of dosimetric materials. In the absence of thermal quenching effects, the TL glow curve is shifted towards higher temperatures when higher heating rates β are used, while the area under the normalized TL signal (TL/β) vs temperature should remain constant and independent of the heating rate. Recent experimental work by Bos et al. (2010) demonstrated the exact opposite effect in the dosimetric material YPO_4:Ce^{3+},Sm^{3+}, in which the area under the normalized curve TL/β vs temperature *increased* with increasing heating rate. Mandowski and Bos (2011) explained this anomalous heating rate effect by using the SLT model developed by Mandowski (2005). Good qualitative agreement was found between the simulated results and experimental data. It is also noted that a similar anomalous heating rate effect was reported by Kitis et al. (2006) for Durango apatite.

The goals of the present paper are to:

(a) Demonstrate that it is possible to describe mathematically the anomalous heating rate effect by using a simplified SLT model.
(b) Investigate the conditions under which the standard methods of TL analysis (initial rise and various heating rate methods), may fail to produce the correct kinetic parameters within this model.
(c) Provide a physical explanation for the underestimation of the activation energy by the variable heating rate method of TL analysis.

The simulations in this paper show that the anomalous heating rate or "anti-quenching" phenomenon can also be described mathematically within this simplified SLT model, as a competition effect between multiple luminescence pathways in luminescence materials. This description is in agreement with the recent explanation given by Mandowski and Bos (2011). Furthermore, it is shown that the variable heating rate method of analysis can systematically underestimate the activation energy E, while by contrast the initial rise method of analysis yields in most cases the correct value for E.

It is emphasized that this paper does not advocate the correctness of one SLT model over others, but rather serves as an initial comparative investigation and demonstration of the anomalous heating rate effect within a simplified SLT model of TL.

1.1. A simplified SLT model of TL

Recently Chen et al. (2012) developed a two-stage TL model in which stimulation of electrons into the conduction band takes place via an intermediate localized excited state. Electrons are thermally stimulated from the trap into an excited state and then thermally released into the conduction band from which they may either be retrapped or recombined with holes in centers. The model of Chen et al. (2012) is based only on recombinations of electrons taking place through the conduction band. These authors solved the differential equations for the process during heating and isothermal decay, and used several analytical methods to determine the effective activation energy E and frequency factor s. Their simulations showed that in many cases the effective activation energy estimated from several methods of TL analysis is equal to $E_1 + E_2$, where E_1 and E_2 are the activation energies for the first and second stage of thermal stimulation. However, unusual cases were also reported in the simulations, in which the effective activation energy is closer to E_1 rather than $E_1 + E_2$.

This paper is based on a simplified SLT model shown in Fig. 1. This model has mathematical similarities with the model developed by Chen et al. (2012). In the simplified SLT model of Fig. 1, an additional non-radiative transition L_B is shown to take place directly from the excited state into the recombination center. However, it must be emphasized that from a physical point of view, the model of Fig. 1 has physical characteristics appropriate for an SLT model, rather than the physical characteristics of the two-stage STM model by Chen et al. (2012). Although in what follows we will use a notation and mathematical formalism similar to the STM model by Chen et al. (2012), it must be kept in mind that Fig. 1 represents a mathematically simplified SLT model.

The kinetic parameters in the model are as follows. The trapping state with concentration N (cm^{-3}) and instantaneous occupancy n (cm^{-3}) is shown, as well as the excited state n_e. The activation energy for thermal excitation into the excited state is E_1 (eV) and the frequency factor is s_1 (s^{-1}). Once the electron is in the excited state, it can either retrap with a probability of p (s^{-1}) or be thermally excited into the conduction band (CB). The activation energy for this transition is E_2 (eV) and the frequency factor is s_2 (s^{-1}). The instantaneous concentration of electrons in the conduction band is denoted by n_c (cm^{-3}). From the conduction band, the electrons can be retrapped into the excited state with a retrapping probability coefficient of A_n ($cm^3\ s^{-1}$), or recombine with a hole in the center with a probability coefficient of A_m ($cm^3\ s^{-1}$). This recombination pathway is assumed to produce the TL photons with an instantaneous intensity $I(t)$, via the radiative transition indicated by L_C in Fig. 1. The added non-radiative transition shown as L_B in Fig. 1 represents the direct *non-radiative* recombination of an electron in the excited state with a hole in the center, with a probability coefficient B (s^{-1}). It is assumed that at the end of the initial excitation by irradiation, the number of trapped holes m_0 is equal to the total number of trapped electrons $n_0 + n_{e0}$. In addition, since the excitation is performed at a relatively low temperature, n_{e0} can be considered to be relatively small so that $n_0 \approx m_0$. As discussed in Chen et al. (2012), the detailed balance principle dictates that the values of the frequency factor for the first transition s_1 and the retrapping probability p must be equal, i.e. $s_1 = p$.

The simultaneous differential equations governing the processes during the heating stage, shown in Fig. 1 are:

$$\frac{dn}{dt} = -s_1 n \exp(-E_1/kT) + p n_e, \tag{1}$$

$$\frac{dn_e}{dt} = A_n(N-n-n_e)n_c + s_1 n \exp(-E_1/kT) - s_2 n_e \exp(-E_2/kT) - p n_e - B n_e, \tag{2}$$

$$I(t) = L_c = A_m m n_c, \tag{3}$$

$$L_B = B n_e, \tag{4}$$

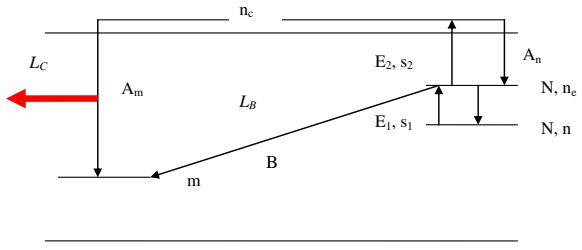

Fig. 1. A simplified SLT model which includes the non-radiative transition L_B. The various parameters and transitions in this model are explained in the text.

$$\frac{dm}{dt} = -A_m m n_c - B n_e, \tag{5}$$

$$\frac{dn_c}{dt} = \frac{dm}{dt} - \frac{dn}{dt} - \frac{dn_e}{dt}. \tag{6}$$

It is noted that the mathematical form of the equations in this paper is rather unusual, when compared with commonly used equations for an SLT or an STM model. For example, the L_B transition in Eq. (4) assumes that each trap has a nearby filled recombination centre, while Eqs. (3) and (5) indicate transitions taking place via the conduction band. The use of these hybrid equations is discussed in some detail in the Discussion section of this paper, where it is argued that the approximate Eqs. (3)–(5) would only be applicable under certain physical conditions, namely that all pairs of donors and acceptors are in close physical proximity, and the concentration of recombination centers remains practically constant through the TL process.

The first term in Eq. (2) is based on the assumption that no retrapping into the excited state n_e is possible if there is an electron either in the ground state of the trap, or in its excited state. Chen et al. (2012) obtained analytical expressions for the TL intensity by assuming that excited states relax quite rapidly compared to the time scales of TL experiments. In analytical form, this assumption can be written as:

$$\frac{1}{n_e}\frac{dn_e}{dt} << s_2 \exp(-E_2/kT) + p + B. \tag{7}$$

By using this approximation in Eq. (2), one solves for n_e:

$$n_e = \frac{A_n(N-n-n_e)n_c + s_1 n \exp(-E_1/kT)}{p + B + s_2 \exp(-E_1/kT)}, \tag{8}$$

and by substituting into Eq. (1) and using the approximation $n \gg n_e$, one obtains:

$$\frac{dn}{dt} = -n s_{eff} \exp[-(E_1+E_2)/kT] + A_{n,eff}(N-n)n_c, \tag{9}$$

where

$$s_{eff} = \frac{s_1 s_2}{p + B + s_2 \exp(-E_2/kT)}, \tag{10}$$

and

$$A_{n,eff} = \frac{p}{p + B + s_2 \exp(-E_2/kT)} A_n. \tag{11}$$

The last two equations are identical to Eqs. (10) and (11) in Chen et al. (2012), with the additional probability coefficient B added in the denominator. Eqs. (10) and (11) look exactly like the conventional one-stage kinetics, except that the rate constants s_{eff} and $A_{n,eff}$ are now temperature dependent and the effective activation energy is $E_1 + E_2$. As discussed in Chen et al. (2012), there are two limiting cases to consider, as follows.

1.1.1. Limiting case #1

In the first case, if

$$s_2 \exp(-E_2/kT) << p + B, \tag{12}$$

then $s_{eff} = s_1 s_2/(p+B) = s_1 s_2/(s_1+B)$ and $A_{n,eff} = A_n p/(p+B) = A_n s_1/(s_1+B)$. Using these approximations, Eq. (9) reduces to

$$\frac{dn}{dt} = -n\frac{s_1 s_2}{s_1 + B}\exp[-(E_1+E_2)/kT] + A_n \frac{s_1}{s_1+B}(N-n)n_c, \tag{13}$$

or

$$\frac{dn}{dt} = \frac{s_1}{s_1+B}[-n s_2 \exp[-(E_1+E_2)/kT] + A_n(N-n)n_c], \tag{14}$$

This equation is identical to Eq. (9) in Chen et al. (2012), but with the TL intensity being multiplied by a constant factor $s_1/(s_1+B)$. Therefore, their previous conclusions remain valid for the extended model of Fig. 1, i.e. one would expect to obtain the effective kinetic parameters $E_1 + E_2$ and s_2. This first limiting case obviously corresponds to the usual assumptions made in a TL model, where s_{eff} and $A_{n,eff}$ are constants.

1.1.2. Limiting case #2

In the second limiting case considered by Chen et al. (2012),

$$s_2 \exp(-E_2/kT) >> p + B. \tag{15}$$

In this case Eqs. (10) and (11) yield the temperature-dependent parameters $s_{eff} = s_1 \exp(E_2/kT)$ and $A_{n,eff} = (p/s_2)\exp(E_2/kT)A_n$. The governing Eq. (9) now becomes

$$\frac{dn}{dt} = -s_1 n \exp(-E_1/kT) + (pA_n/s_2)\exp(E_2/kT)(N-n)n_c. \tag{16}$$

This equation is identical to Eq. (15) in Chen et al. (2012), and their previous conclusions again remain valid. In this second rather unusual case, the relatively small value of $p + B$ in Eq. (15) may yield strange behavior. The exponential temperature dependence of s_{eff} has the effect of reducing the effective energy from $E_1 + E_2$ to E_1, while the effective frequency factor s_{eff} reduces here to s_1. The exponential temperature dependence of $A_{n,eff}$ may also influence the shape of the TL peak.

For values of $p + B$ which are in-between the two limiting cases shown in Eqs. (12) and (15), one would expect an intermediate behavior in the model, namely effective activation energy values between $E_1 + E_2$ and E_1, and effective frequency factors values from s_2 to s_1 correspondingly.

2. Simulation results

2.1. Simulation of the anomalous heating rate effect using the model of Fig. 1

Fig. 2a shows the result of simulating the TL glow peak for four different values $\beta = 1,2,3,4$ K/s of the heating rate, and as a function of *time*. These glow curves are obtained by solving the system of differential Eqs. (1)–(6) with the following values of the kinetic parameters: $p = s_1 = 10^9$ s^{-1}, $s_2 = 10^{12}$ s^{-1}, $A_n = 10^{-8}$ cm^3 s^{-1}, $A_m = 10^{-6}$ cm^3 s^{-1}, $N = 10^{13}$ cm^{-3}, $E_1 = 0.8$ eV, $E_2 = 0.5$ eV. The initial conditions for the heating stage of the simulation are $n_e(0) = n_c(0) = 0$, $n(0) = m(0) = 10^{11}$ cm^{-3} and the probability of localized recombination pathway is set at $B = 10^4$ s^{-1}. Fig. 2a shows that as the heating rate is increased, the height of the TL glow curves increases with time, while the maximum of the TL glow curve shifts towards a higher time t. Fig. 2b shows the same glow curves normalized by dividing them by their corresponding heating rates β. Numerical integration of the normalized TL glow curves in Fig. 2b shows that the integrated area of each curve is constant and independent of the heating rate; in fact, it is found that this integrated area is equal to the initial total concentration

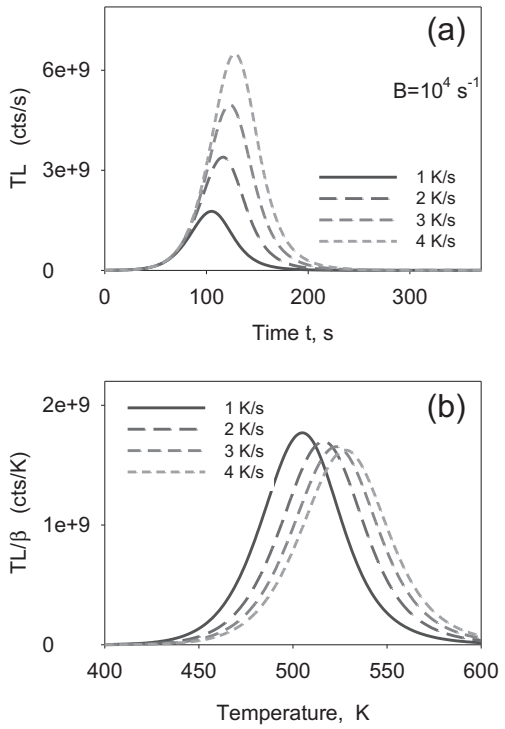

Fig. 2. (a) Simulated TL glow peak for four different values β = 1,2,3,4 K/s of the heating rate, and as a function of *time*. As the heating rate is increased, the height of the TL glow curves increases with time, while the maximum of the TL glow curve shifts towards a higher time t. (b) The same glow curves as in (a), normalized by dividing by with their corresponding heating rates β. The integrated area under all four curves is constant, independent of the heating rate and equal the initial total concentration $n(0) = 10^{11}$ cm^{-3} of trapped electrons at the start of the heating process. The FWHM of the glow curves increases slightly with the heating rate.

$n(0) = 10^{11}$ cm^{-3} of trapped electrons at the start of the heating process. Furthermore, inspection of Fig. 2b shows that the FWHM of the glow curves increases very slightly as a function of the heating rate, from 61 K at the lowest heating rate of 1 K/s, up to 64 K for the highest heating are of 4 K/s. This slight increase of the FWHM combined with the slight decrease of the height of the TL glow curves in Fig. 2b, to result in a constant area under the curves. Overall, the simulated results of Fig. 2 are not surprising, and they are expected on the basis of well-known theories of TL. In the example of Fig. 2, the coefficient B is rather small, and the non-radiative pathway L_B has no appreciable effect on the TL glow curves.

The simulations in Fig. 2 are next repeated using the same parameters, but with the parameter B increased to $B = 10^7$ s^{-1}, with the results for the normalized TL glow curves L_C/β shown in Fig. 3a. These simulated TL glow curves clearly demonstrate the anomalous heating rate phenomenon observed in the dosimetric material YPO_4 double doped with lanthanides, and they are similar to the glow curves simulated by Mandowski and Bos (2011) using a more complex type of SLT model. Fig. 3b shows the corresponding normalized non-radiative intensity L_B/β, calculated using Eq. (4). Fig. 3c shows the integrated areas L_C/β, L_B/β and their sum as a function of heating rate.

Fig. 3c shows that as the heating rate increases, the area of the L_C/β glow curves increases, while the corresponding area of the L_B/β curves decreases. The total sum of these areas $L_C/\beta + L_B/\beta$ remains constant and is equal to the initial total concentration $n(0) = m(0) = 10^{11}$ cm^{-3} of trapped electrons. The increase of the FWHM at higher heating rates shown in Fig. 3a is in qualitative agreement with the experimental results shown for example in Mandowski and Bos (2011).

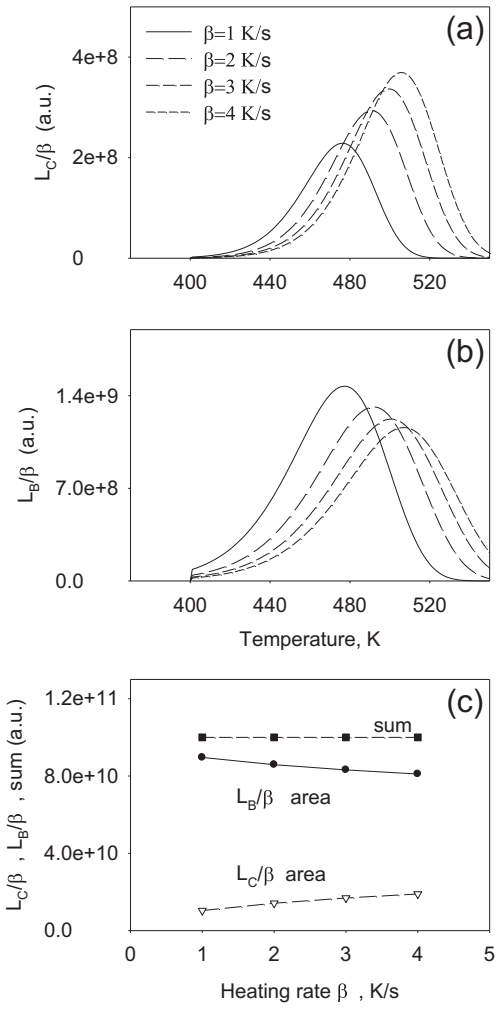

Fig. 3. (a) The simulations in Fig. 2 are repeated with a higher value of the parameter $B = 10^7$ s^{-1}. The normalized curves L_C/β shown here demonstrate the anomalous heating rate phenomenon. The FWHM increases at higher heating rates, in agreement with the experimental results discussed in the text. (b) The corresponding normalized non-radiative quantity L_B/β, calculated using Eq. (4). As the heating rate increases, the area of the L_C/β glow curves in (a) increases, while the corresponding area of the L_B/β curves decreases. The total sum of these areas $L_C/\beta + L_B/\beta$ remains constant (c) The integrated areas L_C/β, L_B/β from (a) and (b), and their sum as a function of heating rate.

The results of Fig. 3 show that the physical basis of the simulated anomalous heating rate effect is a competition between the radiative and non-radiative pathways of the system. Competition for available charges between the two pathways causes the L_C/β area to increase, while the corresponding L_B/β areas must decrease by the same amount because of charge conservation. These results also indicate that the value of the recombination coefficient B in the model is correlated to the anomalous heating rate effect. One might expect on physical grounds that the anomalous heating rate effect will become more dominant as B increases. This relationship between B and the anomalous heating rate is shown more clearly in Fig. 4, in which the TL glow curves are simulated for four different values of $B = 10^4, 10^5, 2 \times 10^6, 10^7$ s^{-1}. Fig. 4a and b shows that for low values of B the simulated glow curves show "normal" TL behavior, with the area under the glow curves remaining constant at different heating rates. Close inspection shows that there is little change of the four glow curves for $B < 10^5$ s^{-1}. However, Fig. 4c and d shows that for values of $B > 10^5$ s^{-1} the glow curves show the anomalous heating rate effect, with the normalized area under the glow curves increasing with the heating rate. Comparison of Fig. 4c

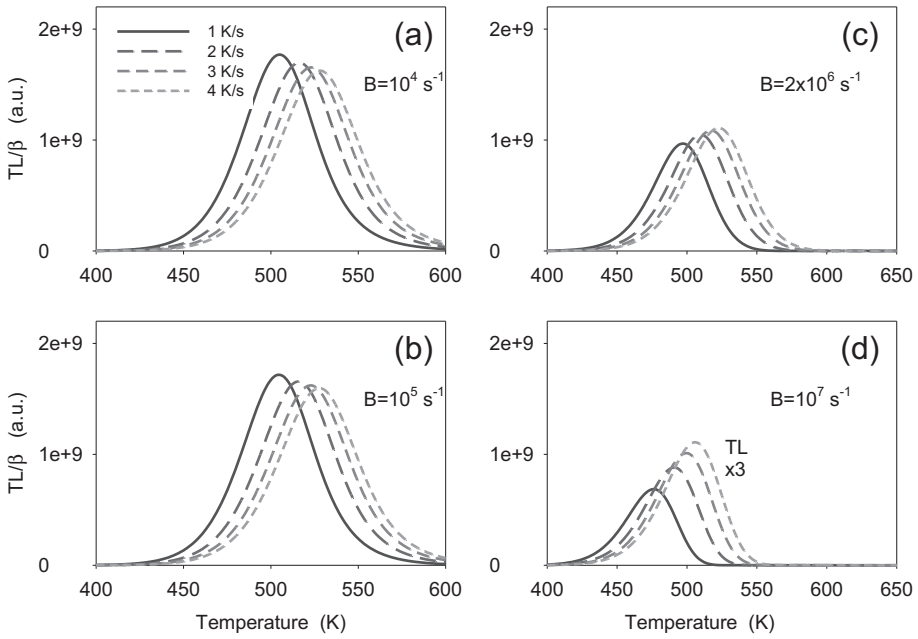

Fig. 4. Simulated TL glow curves for four different values of $B = 10^4, 10^5, 2 \times 10^6, 10^7\ s^{-1}$. (a) and (b): For low values of B the simulated glow curves show "normal" TL behavior, with the area under the glow curves remaining constant at different heating rates. There is little change in the four simulated glow curves for $B < 10^5\ s^{-1}$. (c) and (d): For high values of B the glow curves show the anomalous heating rate effect, with the normalized area under the glow curves increasing with the heating rate. The higher the value of B, the more pronounced is the anomalous increase in the area under the glow curves.

and d shows that the higher the value of B, the more pronounced is the anomalous increase in the area under the glow curves. At the same time the overall intensity of the TL glow curves decreases as the value of B is increased, due to increased competition from the non-radiative luminescence pathway.

Two important practical questions that the model could help elucidate are:

(a) What effect do these competition effects (and the value of B) have on the shape of the TL glow curves?
(b) Can the activation energy E be extracted reliably from the shape of the simulated TL glow curves by using standard methods of TL analysis?

In order to answer these important practical questions, two standard methods of analysis of TL glow curves are simulated in the next section, namely the initial rise and the various heating rate methods of TL analysis. For simplicity, these two methods will be referred to as the IR and VHR methods in the rest of this paper.

2.2. The initial rise and various heating methods of TL analysis

When applying the VHR method of analysis to TL glow curves, one plots $\ln(T_m^2/\beta)$ vs $1/kT_m$, where T_m is the temperature of maximum TL intensity and k is the Boltzmann constant. The slope of the linear graph obtained in this manner is equal to the activation energy E, while the y-intercept of this graph yields the frequency factor s. Specifically the y-intercept is given by the expression $\ln(E/sk_B)$, where k_B is the Boltzmann constant. In the IR method of TL analysis, one plots the natural logarithm $\ln(I)$ of the intensity $I(T)$ in the initial part of the TL glow curve, as a function of $1/kT$. Here T is the temperature corresponding to the intensity $I(T)$. The slope of the resulting linear graph is equal to $-E$.

Fig. 5a shows a comparison of the TL glow curves obtained with two values of $B = 10^5\ s^{-1}$ and $B = 2 \times 10^6\ s^{-1}$. It is clearly seen that as the value of B is increased (dashed line), the shape of the TL glow

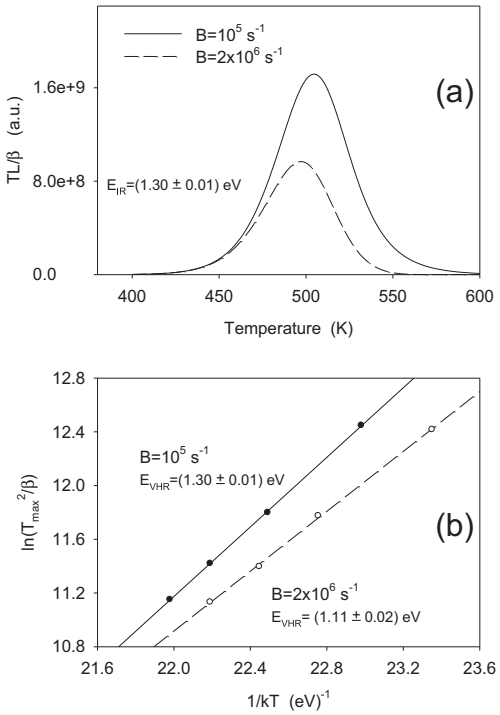

Fig. 5. (a) Comparison of the TL glow curves obtained with two values of $B = 10^5\ s^{-1}$ (solid line) and $B = 2 \times 10^6\ s^{-1}$ (dashed line). As the value of B is increased the shape of the TL glow curve remains the same at low temperatures but becomes distorted at the higher temperatures of the glow peak. Application of the IR method to both glow curves yields the same value of $E_{eff} = (1.30 \pm 0.01)$ eV. (b) Application of the VHR method of analysis to the case of low value of $B = 10^5\ s^{-1}$ (solid line) yields the effective activation energy $E_{eff} = E_1 + E_2 = (1.30 \pm 0.01)$ eV. In the case of the higher value of $B = 2 \times 10^6\ s^{-1}$ (dashed line) the VHR method yields a much smaller value of $E_{eff} = E_1 + E_2 = (1.11 \pm 0.02)$ eV.

curve remains the same at low temperatures located on the rising part of the TL glow curve. As a result of the similarity of the two glow curves at low temperatures, application of the IR method to both glow curves yields the same value of $E_{eff} = (1.30 \pm 0.01)$ eV. However, Fig. 5a shows that increasing the value of B results in a distortion of the shape of the glow curve at higher temperatures, in a reduction of the TL height, and in a shift of the glow curve maximum towards lower temperatures. As a result of these distortions taking place in the shape of the glow curve, application of the VHR method of analysis to the two TL glow curves in Fig. 5a yields different values of E_{eff}. Specifically, Fig. 5b shows that in the case of low value of $B = 10^5$ s^{-1} (solid line) the VHR method yield the same value of effective activation energy as the IR method, namely $E_{eff} = E_1 + E_2 = (1.30 \pm 0.01)$ eV. However, for the higher value of $B = 2 \times 10^6$ s^{-1} (dashed line) the VHR method yields a much smaller value than the IR method, i.e. $E_{eff} = (1.11 \pm 0.02)$ eV.

The variation of the effective parameters E_{eff} and s_{eff} with the parameter B is shown in a systematic manner in Fig. 6. For low values of $B < 10^6$ s^{-1}, both the VHR method and the IR method yield the limiting value of $E_{eff} = E_1 + E_2 = 1.3$ eV. By contrast, for high values of $B > 10^6$ s^{-1} the VHR method underestimates the activation energy, and E_{eff} tends towards the limiting value $E_{eff} = E_1 = 0.8$ eV. However, the IR method yields the same limiting value of $E_{eff} = E_1 + E_2$ at all values of B. Fig. 6b shows the calculated values of the effective frequency factor s_{eff}, which are obtained from the y-intercept of the VHR method. As may have been expected, for low values of B the frequency factor $s_{eff} \sim s_2 = 10^{12}$ s^{-1}, while for high values of B one obtains $s_{eff} \sim s_1 = 10^9$ s^{-1}, as discussed in Chen et al. (2012).

The results in Fig. 6 indicate that the use of the IR method may be more reliable than the VHR method for extracting the activation energy E, especially in materials in which strong competition exists between radiative and non-radiative pathways.

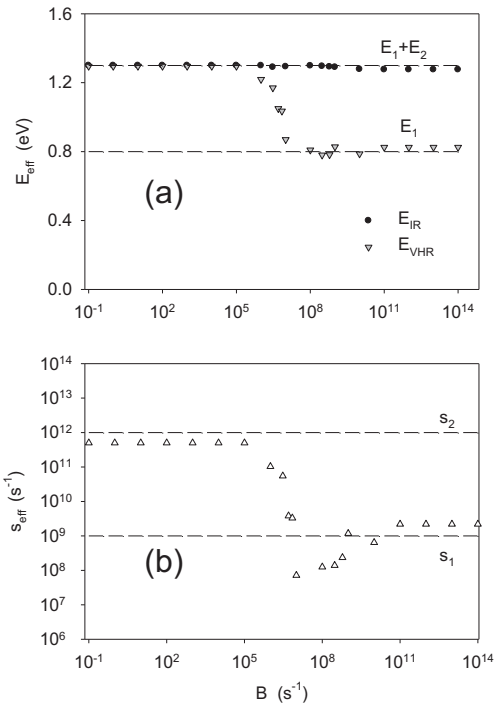

Fig. 6. Variation of the effective kinetic parameters (a) E_{eff} and (b) s_{eff} with the parameter B. For low values of $B < 10^6$ s^{-1}, both the VHR method and the IR method yield the limiting value of $E_{eff} = E_1 + E_2 = 1.3$ eV. For high values of $B > 10^6$ s^{-1} the VHR method underestimates the activation energy, with E_{eff} tending towards the limiting value $E_{eff} = E_1 = 0.8$ eV. However, the IR method yields the same limiting value of $E_{eff} = E_1 + E_2$ at all values of B.

In the next subsection a systematic study is carried out of the dependence of the effective activation energy E_{eff} on the various kinetic parameters in the model.

2.3. Dependence of the activation energy E_{eff} on the kinetic parameters used in the model

In this section the dependence of the anomalous heating rate effect on the chosen values of the kinetic parameters is studied in a systematic manner, by allowing random variations of the kinetic parameters in the model within physically reasonable values. This method of analysis was used recently by Pagonis and Kitis (2012) to explain the prevalence of first order kinetics in TL dosimetric materials. The main advantage of this method of random variations is that the average behavior of a natural material can perhaps be simulated more accurately, and for a very wide range of the kinetic parameters.

In a real dosimetric material one can expect random variations of the recombination and retrapping coefficients, as well as random variations in the concentrations and filling of the traps. Such random variations would lead to statistical variations between different samples of the same material, and even in significant differences between aliquots of the same sample. Pagonis and Kitis (2012) simulated the random natural variations of the recombination and retrapping coefficients and of the initial concentrations of traps in the interactive multitrap trap system of TL, by allowing these parameters to vary between physically reasonable minimum and maximum values. These authors noted that recombination and retrapping coefficients, (A_m, A_n) in Fig. 1, have been measured for only a few dosimetric materials (Lax, 1960), and that their range is believed to be as low as 10^{-10} cm^3 s^{-1} and as high as 10^{-5} cm^3 s^{-1} (Chen and Pagonis, 2011). Since these values represent a span of 5 orders of magnitude, one should allow random uniform variations in their *logarithms*, rather than in the values themselves. Similarly, the initial concentration of filled traps $n(0)$ is allowed to vary from a low value of 0.001 N (0.1% filled trap ratio), to a high value of 0.97 N (97% filled traps). The three parameters A_m, A_n, and $n(0)$ were varied randomly within these broad physical limits, and the logarithm of the total trap concentration N was also varied randomly between $N = 10^{12}$ cm^{-3} and 10^{15} cm^{-3}. The kinetic parameters that characterize the two-stage TL process in Fig. 1 are kept fixed as in the previous simulations in this paper, namely $s_1 = 10^9$ s^{-1}, $s_2 = 10^{12}$ s^{-1}, $E_1 = 0.8$ eV, $E_2 = 0.5$ eV.

Fig. 7 shows the results of simulating $M = 2000$ random variants of the model in Fig. 1, produced in the above manner, with a constant value of coefficient $B = 10^8$ s^{-1}. Fig. 7a and b shows the distribution of the activation energies E_{IR} and E_{VHR} obtained with the IR and VHR methods for a heating rate $\beta = 1$ K/s, with mean values of (1.23 ± 0.03) eV (1σ) and (0.80 ± 0.04) eV (1σ) correspondingly. Similarly, Fig. 7c shows the corresponding distribution of the FWHM of these TL glow curves, with a mean value of (36 ± 1) K (1σ), while Fig. 7d shows the simulated distribution of the temperature of maximum TL intensity T_{max}, with a mean value of (461 ± 6) K (1σ).

Overall, the results shown in Fig. 7 are rather remarkable. They indicate strongly that the average position and average shape of the TL glow peak are determined almost exclusively by the parameters s_1, s_2, E_1, E_2. Random variations of the additional parameters A_m, A_n, N, $n(0)$ within many orders of magnitude, have little effect on the average shape and position of the glow peak.

These simulated results were verified by running the simulation with $M = 10^4$ random variants of the model. This resulted in a small change of the order of 1% or less in the average values of the parameters, and in little apparent change of the overall shape of the histograms. The main result of using more natural variants in the

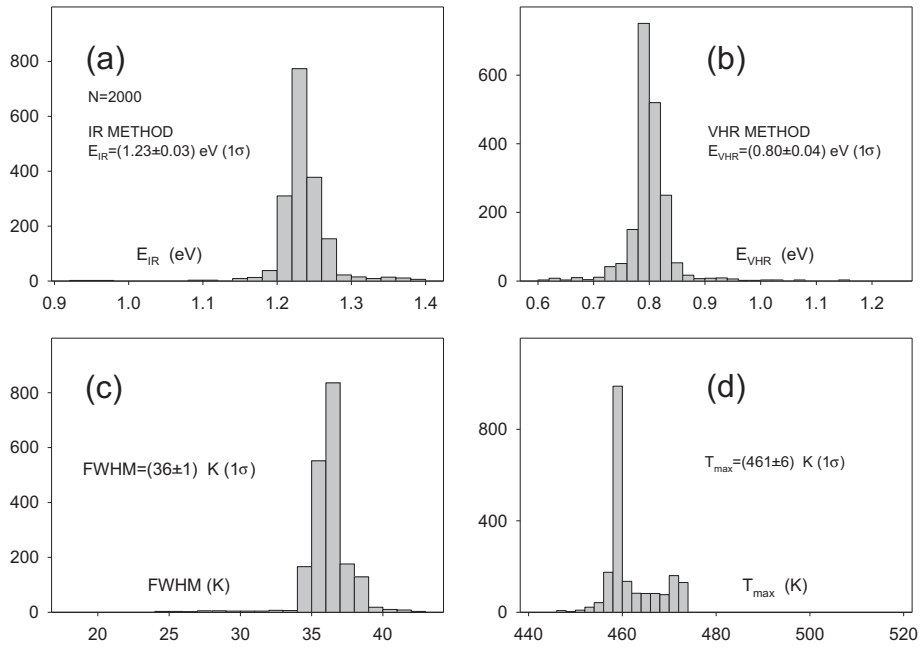

Fig. 7. The distribution of the activation energies (a) E_{IR} and (b) E_{VHR} obtained with the IR and VHR methods. $M = 2000$ variants of the model are simulated, as discussed in the text. (c) and (d) show the distribution of the FWHM and temperature of maximum TL intensity T_{max} of $M = 2000$ variants when the heating rate is $\beta = 1$ K/s. These results show that the average shape of the TL glow peak is determined almost exclusively by the parameters s_1, s_2, E_1, E_2. Random variations of the additional parameters in the model within many orders of magnitude, have little effect on the average shape and position of the glow peak.

simulation was mostly to "smooth out" the histograms, without changing significantly the accuracy and precision of the simulated results. It is concluded that the conclusions drawn from the simulations shown in Fig. 7 are independent of the number of natural variants M used in the simulations.

The simulations shown in Fig. 6 were repeated for $M = 1000$ variants of the model and for different values of the recombination coefficient B, with the average results shown in Fig. 8. As in the case of Fig. 6, it was found that for low values of $B < 10^5$ s^{-1}, both the VHR method and the IR method yield the limiting value of $E_{eff} = E_1 + E_2$. For high values of $B > 10^5$ s^{-1} the VHR method underestimates the activation energy and E_{eff} tends towards the limiting value $E_{eff} = E_1 = 0.8$ eV. By contrast, the IR method yields the limiting value of $E_{eff} = E_1 + E_2$ at all values of B. Once more, the results in Fig. 8 indicate that the IR method may be more reliable than the VHR method for extracting the effective activation energy E.

Fig. 8 presents a clear demonstration that the value of B is the critical parameter determining the average behavior of the system. At low B values the modeled system tends towards the two-stage delocalized behavior, while at high B values it tends towards the localized behavior. It is noted that the error bars shown in Fig. 8 represent the standard deviations (1σ) values of $M = 1000$ variants; the actual error bars for the standard error of the average values of E are much smaller and equal to $\sigma/\sqrt{M}$; these error bars would be barely visible in the data of Fig. 8.

Our preliminary simulations of the VHR effect using the Mandowski (2008) model, show similar results to the graph shown in Fig. 8. Specifically in the presence of strong competing luminescence pathways within the Mandowski model, the VHR method systematically underestimates the activation energy E, while the IR method tends to produce the same E value in most situations. The exact conditions under which these preliminary results hold within the Mandowski model are beyond the purpose of this paper, and a more detailed study needs to be carried out in a systematic fashion.

2.4. Discussion: the anomalous heating rate effect in $YPO_4:Ce^{3+},Sm^{3+}$

In a recent paper Mandowski and Bos (2011) explained the anomalous heating rate dependence of thermoluminescence in $YPO_4:Ce^{3+},Sm^{3+}$, by using the Mandowski SLT model. Their energy scheme is based on the Dorenbos model (2003), on experimental measurements of Poolton et al. (2010), and further simplifications by Bos et al. (2010). Irradiation creates electron hole pairs, with the holes captured at cerium sites and the electrons at Samarium sites. Bos et al. (2010) suggested that recombination in this material takes place in a complex manner via non-radiative tunneling, thermally assisted tunneling and conduction band pathways. The modeling work by these authors successfully explained the broad glow curves

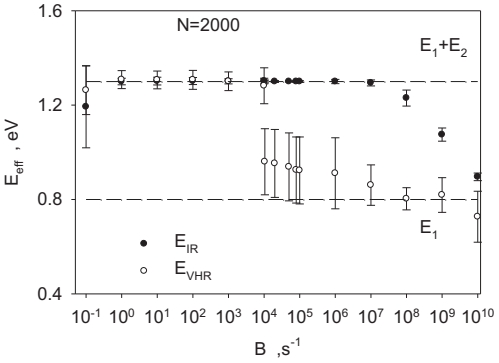

Fig. 8. Average results for $M = 2000$ simulated variants of the model, and for different values of the recombination coefficient B. Similarly to the results of Fig. 6, for low values of B both the VHR method and the IR method yield the limiting value of $E_{eff} = E_1 + E_2$. For high values of B the VHR method underestimates the activation energy and E_{eff} tends towards the limiting value $E_{eff} = E_1 = 0.8$ eV, while the IR method yields the limiting value of $E_{eff} = E_1 + E_2$ at all values of B. The error bars shown here are the standard deviations (1σ); the standard *errors* are than the size of the symbols used for the data points.

and an extra peak apparent at low heating rates, even though the data is rather noisy. These extra small peaks are believed to be the results of a two-stage process, and are an important experimental feature of the TL glow curves in these materials. The physical explanations offered for the anomalous heating rate effect within the model of Mandowski and Bos (2011), is rather similar to the one offered by the model in this paper. These authors point out that as the heating rate is increased, the relative ratio of radiative and non-radiative transitions increases, due to the two-stage process of excitation of charge carriers from traps.

It is noted that the mathematical form of the equations in this paper may appear puzzling when they are considered within an SLT or an STM model. Specifically, the L_B transition as written in Eq. (4) assumes that each trap has a nearby filled recombination centre. This would appear to contradict the conduction band transitions indicated in Eqs. (3) and (5). Although this would appear to be a contradiction between the SLT and STM nature of the model, one can view the model in this paper as a hybrid type of model which would be applicable under certain physical conditions. In essence, this model can be considered a mathematical approximation of the much more complex SLT model formulated by Mandowski (2005). One can envision a physical situation that corresponds to the kinetics shown in Fig. 1 as pairs of donors and acceptors located in close physical proximity, resulting in localized transitions taking place (as in LT models). However, within the statistical ensembles of these donor/acceptor pairs there will be also a finite probability for some of the electrons in the ensemble to participate in transitions involving the conduction band (as in STM models). Overall, one could envision the model of Fig. 1 as representing the probability of various possible transitions occurring within a statistical ensemble, with the competing transition probabilities resulting in the anomalous heating rate effect. From a dosimetry point of view, one might expect the mathematical situation shown in Fig. 1 to occur in a material in which the concentration of recombination centers remains practically constant through the TL process, i.e. the concentration of electrons is much smaller than the corresponding concentration of holes. It is noted that recently Jain et al. (2012) considered a similar physical assumption of constant concentration of holes, in their description of luminescence processes in feldspars, based on localized transitions taking place via tunneling processes.

3. Conclusions

In this paper we demonstrated the anomalous heating rate effect by using a simplified SLT model with mathematical similarities to the two-stage model by Chen et al. (2012). The simplified SLT formulation contains a transition from the excited state of the electron trap directly into the luminescence center. This modified SLT model is somewhat simpler than the Mandowski model, and physically somewhat more intuitive. In addition, it is possible to arrive at analytical expressions for the TL peaks, as was done by Chen et al. (2012). Even though the physical principle behind the two models is similar, there are fundamental differences between the two types of model. Most importantly, the presence of the smaller displacement peaks in the TL glow curves can only be explained by the complex Mandowski model. The present model serves as an initial comparative investigation and demonstration of the anomalous heating rate effect within a mathematically simplified SLT model of TL.

Both the model of Mandowski and Bos (2011) and the model presented in this paper are a simplification of a more complex physical situation. Specifically both models are based on the assumption that the probability of non-radiative recombination B is constant, an assumption that most likely needs to be modified for real dosimetric materials. This recombination probability is most likely a function of the distance between defects involved in the TL process, and improved models of the anomalous heating rate effect should contain such a variable parameter B.

Clearly additional experimental and simulation work needs to be carried out for YPO_4:Ce^{3+},Sm^{3+} and similar materials, in order to ascertain the underlying mechanism for the anomalous heating rate effect. It is suggested that the available experimental TL glow curves from these double doped materials be re-examined, in order to establish whether real differences exist between the E values obtained using the IR and VHR methods.

References

Bos, A.J.J., Poolton, N.R.J., Wallinga, J., Bessière, A., Dorenbos, P., 2010. Energy levels in YPO4:Ce^{3+}, Sm^{3+} studied by thermally and optically stimulated luminescence. Radiat. Meas. 45, 343–346.

Chen, R., Pagonis, V., 2011. Thermally and Optically Stimulated Luminescence: A Simulation Approach. Wiley and Sons, Chichester.

Chen, R., Lawless, J.L., Pagonis, V., 2012. Two-stage thermal stimulation of thermoluminescence. Radiat. Meas. 47, 809–813.

Dorenbos, P., 2003. Relation between Eu^{2+} and Ce^{3+} 4d-transition energies in inorganic compounds. J. Phys. Condens. Matter 15, 8417–8434.

Horowitz, Y.S., Oster, L., Biderman, S., Einav, Y., 2003. Localized transitions in the thermoluminescence of LiF: Mg, Ti: potential for nanoscale dosimetry. J. Phys. D: Appl. Phys. 36, 446–459.

Jain, M., Guralnik, B., Andersen, M.T., 2012. Stimulated luminescence emission from localized recombination in randomly distributed defects. J. Phys. Condens. Matter 24, 385402.

Kitis, G., Polymeris, G.S., Pagonis, V., Tsirliganis, N., 2006. Thermoluminescence response and apparent anomalous fading factor of Durango fluorapatite as a function of the heating rate. Phys. Stat. Sol. (a) 203 (15), 3816–3823.

Kumar, M., Kher, R.K., Bhatt, B.C., Sunta, C.M., 2006. Thermally stimulated luminescence arising simultaneously from localized and delocalized recombination processes. J. Phys. D: Appl. Phys. 39, 2670–2679.

Kumar, M., Kher, R.K., Bhatt, B.C., Sunta, C.M., 2007. A comparative study of the models dealing with localized and semi-localized transitions in thermally stimulated luminescence. J. Phys. D: Appl. Phys. 40, 5865–5872.

Lax, M., 1960. Cascade capture of electrons in solids. Phys. Rev. 119, 1502–1523.

Mandowski, A., Bos, A.J.J., 2011. Explanation of anomalous heating rate dependence of thermoluminescence in YPO4:Ce^{3+}, Sm^{3+} based on the semi-localized transition (SLT) model. Radiat. Meas. 46, 1376–1379.

Mandowski, A., 2005. Semi-localized transitions model for thermoluminescence. J. Phys. D: Appl. Phys. 38, 17–21.

Mandowski, A., 2006. Topology-dependent thermoluminescence kinetics. Radiat. Prot. Dosim. 119, 23–28.

Mandowski, A., 2008. Semi-localized transitions model-General formulation and classical limits. Radiat. Meas. 43, 199–202.

Pagonis, V., Kitis, G., 2012. Prevalence of first order kinetics in thermoluminescence materials: an explanation based on multiple competition processes. Phys. Stat. Sol. (b) 249, 1590–1601.

Pagonis, V., Kulp, C., 2010. Simulations of isothermal processes in the semilocalized transition (SLT) model of thermoluminescence (TL). J. Phys. D: Appl. Phys. 43 (175403), 8.

Pagonis, V., 2005. Evaluation of activation energies in the semi-localized transition model of thermoluminescence. J. Phys. D: Appl. Phys. 38, 2179–2186.

Poolton, N.R.J., Bos, A.J.J., Jones, G.O., Dorenbos, P., 2010. Probing electron transfer processes in YPO4:Ce, Sm by combined synchrotron-laser excitation spectroscopy. J. Phys. Condens. Matter 22 (185403), 12.